

Experimental and analytical investigation on seismic behavior of RC framed structure by pushover method

Akanshu Sharma^{*1,2}, G.R. Reddy¹, R. Eligehausen² and K.K. Vaze¹

¹Reactor Safety Division, Bhabha Atomic Research Centre, Mumbai - 400085, India

²Institute for Construction Materials, University of Stuttgart, Stuttgart - 70569, India

(Received June 16, 2010, Accepted April 14, 2011)

Abstract. Pushover analysis has gained significant popularity as an analytical tool for realistic determination of the inelastic behaviour of RC structures. Though significant work has been done to evaluate the demands realistically, the evaluation of capacity and realistic failure modes has taken a back seat. In order to throw light on the inelastic behaviour and capacity evaluation for the RC framed structures, a 3D Reinforced concrete frame structure was tested under monotonically increasing lateral pushover loads, in a parabolic pattern, till failure. The structure consisted of three storeys and had 2 bays along the two orthogonal directions. The structure was gradually pushed in small increments of load and the corresponding displacements were monitored continuously, leading to a pushover curve for the structure as a result of the test along with other relevant information such as strains on reinforcement bars at critical locations, failure modes etc. The major failure modes were observed as flexural failure of beams and columns, torsional failure of transverse beams and joint shear failure. The analysis of the structure was by considering all these failure modes. In order to have a comparison, the analysis was performed as three different cases. In one case, only the flexural hinges were modelled for critical locations in beams and columns; in second the torsional hinges for transverse beams were included in the analysis and in the third case, joint shear hinges were also included in the analysis. It is shown that modelling and capturing all the failure modes is practically possible and such an analysis can provide the realistic insight into the behaviour of the structure.

Keywords: reinforced concrete structure; experiment; pushover analysis; failure modes; seismic response

1. Introduction

As more and more emphasis is being laid on nonlinear analysis of RC framed structures subjected to earthquake excitation, the research and development on both nonlinear static (pushover) analysis as well as nonlinear dynamic (time history) analysis is in the forefront. Nonlinear static pushover analysis has become a popular analysis tool for seismic assessment of reinforced concrete structures. The method provides a good insight into the load capacity, deflection behavior, failure modes, inelastic excursions and progressive collapse etc, while at the same time being much less prohibitive from the point of view of computational cost as compared to nonlinear dynamic analysis. Standards/

*Corresponding author, Scientific Officer BARC and Visiting Researcher Univ. of Stuttgart,
E-mail: akanshu@barc.gov.in; akanshusharma@yahoo.co.in

guidelines such as ATC 40 (ATC 1996), FEMA 273 (BSSC 1997) followed by FEMA 356 (FEMA 2000) have given detailed guidelines to perform the nonlinear static pushover analysis and to use it to obtain the performance of the structures under a given earthquake scenario. The most recent update in this line is FEMA 440 (ASCE 2005) that is an outcome of ATC-55 project. The post processing procedures recommended, to determine the performance of the structure against a given earthquake, are different for different codes with ATC 40 recommending capacity spectrum method, FEMA 356 describing displacement coefficient method and FEMA 440 describing improvements to both capacity spectrum and displacement coefficient methods. The basic input required by the analysis methods recommended by these guidelines is the base shear v/s roof deflection plot popularly known as capacity curve or pushover curve. The capacity of the structure represented by this capacity curve is then compared with the seismic demand, often represented by a demand spectrum following one of the various recommended procedures such as capacity spectrum method, displacement coefficient method etc. This highlights the importance of the correct determination of the load-deflection response of the structure, since the accuracy of the performance determination is then mainly dependent on the accuracy of capacity determination of the structure.

In order to capture the complete picture of the nonlinear behavior of the frame structure, it is required to have correct models for the members such as beams, columns under the bending moments, shear forces, axial forces and torsional moments along with interactions and also models that can predict more complex behavior at the connections e.g., joint shear failure, bond failure etc. Especially, for the structures those were designed and detailed as per the non-seismic detailing practice, the nonlinear behavior of the beam-column joints play a very dominant role in determining the seismic response of the structure. The modeling of inelastic behavior of the members under flexure, shear, torsion and axial forces are very well documented and several models and methods are available in the literature to model such characteristics (Park and Paulay 1975, Samra 1980, Paulay and Priestley 1992, Watanabe and Lee 1998). Consequently, mostly while analyzing a structure by pushover method, only member nonlinearities are considered and the joints are assumed as rigid. However, few authors have introduced a joint element to account for inelastic shear deformation and bar bond slip (Biddah and Ghobarah 1999, Ziyaeifara and Noguchib 2000, Cosenza *et al.* 2006).

The correct procedure to evaluate the characteristics can be judged by comparing the analytical results with those of the experiments. In recent past, many attempts have been made to prove the efficacy of pushover method both analytically (Chopra and Goel 2002, 2004, Isakovic and Fischinger 2006, Paraskeva *et al.* 2006, Han and Chopra 2006, Kafrawy *et al.* 2011) and experimentally (Weng *et al.* 2006, Ludovico *et al.* 2008). The references are only indicative and not exhaustive.

In this work, seismic pushover experiment was conducted on a three storied, 3D RC framed structure designed as per non-seismic rules, under lateral monotonic pushover type loads. The failure patterns included the flexural failure of beams and columns, torsional failure of beams transverse to loading direction and joint shear failures. The capacity curve for the structure was obtained in the experiment along with several other data providing the information on the strains in re-bars, failure modes, deflection profiles etc. Analysis of the structure was performed giving considerations to different kinds of nonlinearities, one at a time and the usefulness of relatively simple but accurate procedures was displayed.

2. Research objectives

Many researchers have pursued research to improve the predictions of demand on the structure (Chopra and Goel 2002, 2004, Fajfar 1996, 2000, Kilar and Fajfar 1996, 1997, 2001, Antoniou and Pinho 2004, Kunnath 2004, Isakovic and Fischinger 2006, Paraskeva *et al.* 2006, Han and Chopra 2006, Kafrawy *et al.* 2011). However, the evaluation of capacity is considered more or less for granted. To obtain results in a reasonable time constraint, engineers make certain assumptions e.g. with respect to the influential failure modes and thus, only certain nonlinearities are modeled and considered most popular of which are the flexural characteristics of the members, while the other more complex phenomena such as torsion behavior and joint shear failure are in general neglected. Such assumptions greatly influence the results obtained from the analysis especially if the structure is not specially designed and detailed for seismic considerations. In this work, a three storied, 3D structure was tested and analyzed under monotonically increasing lateral pushover loads. Behavior of such structures under earthquakes is highlighted by various failure modes and it is shown that modeling of all the possible failure modes is important to capture the true and complete behavior of the structure.

3. Description of structure

3.1 Geometry

The structure tested was a three storey structure with a column height of 1.8 meters. The plan dimensions were 3 m × 3 m, with bay width of 1.5 meters in both directions. Fig. 1 shows the general geometric arrangement of the structure. The grids are named as A, B, C and 1, 2, 3 for easy identification of the columns later. The typical beam and column size was 150 mm × 200 mm and the slab thickness was 100 mm. In Fig. 1, the longitudinal reinforcement for the beams is mentioned in the “number of bars – diameter of bars in mm, e.g., 2-16 refers to 2 number of 16 mm diameter bars. The transverse reinforcement is mentioned in “diameter of stirrups/ties (in mm) – spacing of stirrups/ties (in mm), e.g., 6-150 refers to 6 mm diameter bars as stirrups/ties spaced at a centre to centre spacing of 150 mm. The base raft was 275 mm thick and was provided with PVC sleeves at a grid spacing of 1000 mm to allow for fixing the raft to strong floor with bolts.

3.2 Material properties

The concrete mix used for the construction of the structure was design mix to achieve a characteristic strength (95 percentile value) of 25 MPa, with a ratio of 1:2.28:2.78 for Cement: Fine Aggregates: Coarse Aggregates and a water-cement ratio of 0.4. Super-plasticizers were added to the mix to improve workability. High Yield Strength Deformed (HYSD) bars with specified characteristic yield strength of 415 MPa were used as reinforcement.

The actual material properties from tests were found as

Average Concrete Strength: 34 MPa

Average Reinforcement yield stress: 478 MPa

Average Reinforcement ultimate stress: 665 MPa

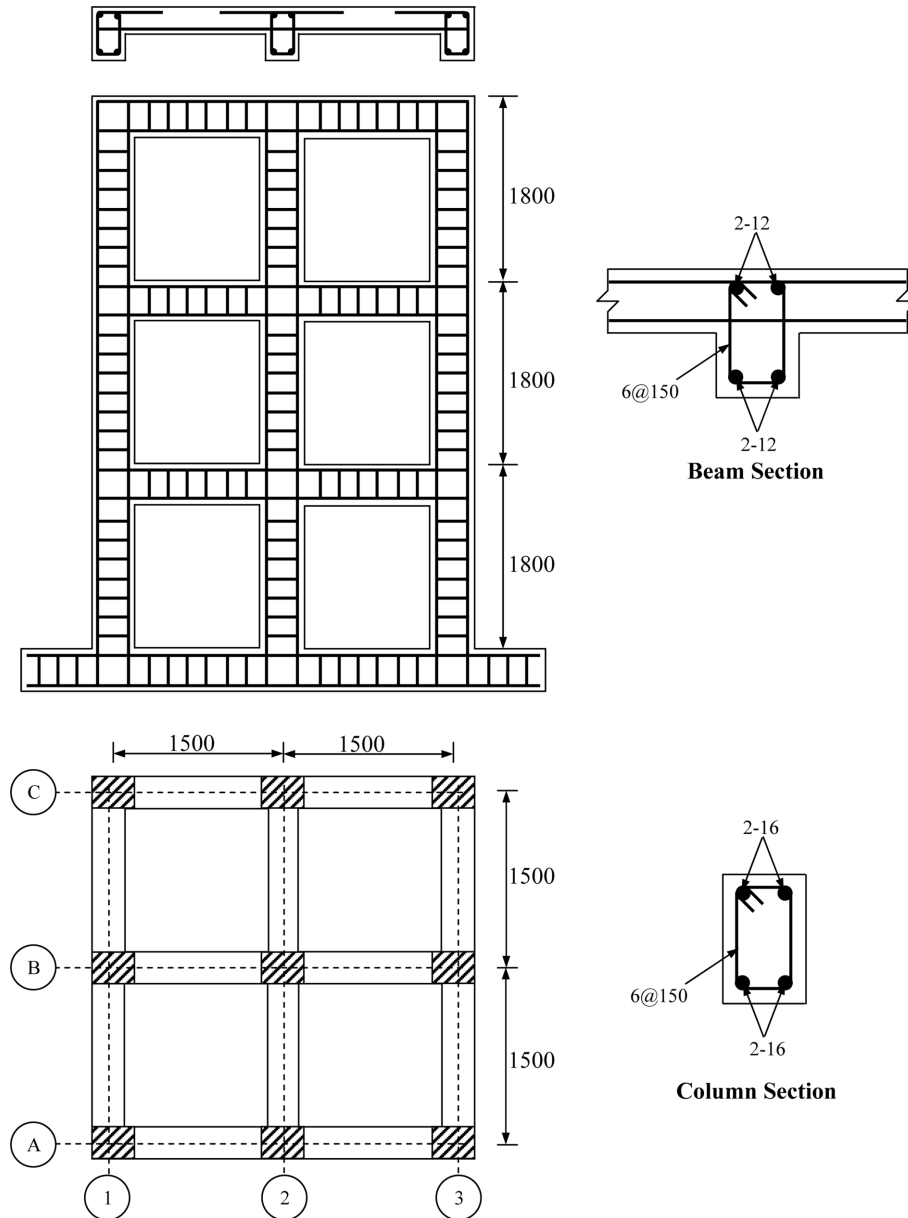


Fig. 1 Description of structure

4. Experimental setup, instrumentation and loading pattern

The structure, as described was tested at the ASTaR lab of the Structural Engineering Research Centre (SERC) Chennai. Fig. 2 shows the experimental setup of the structure. Additional masses of 0.54 tonnes were kept on each floor. Static loads were applied through hydraulic jacks at three levels of the structure in a predefined parabolic pattern with a load ratio of P: 4P: 9P for 1st floor: 2nd floor: 3rd floor. The hydraulic jacks were connected to the heavy duty reaction wall on one end



Fig. 2 Experimental setup for the structure

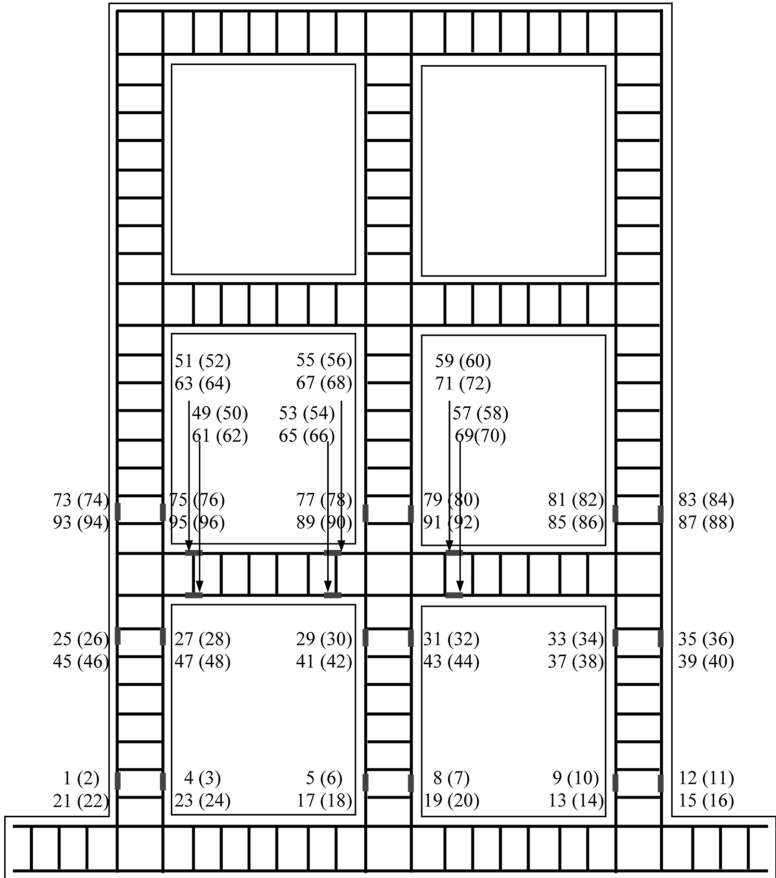


Fig. 3 Location of strain gauges on reinforcement bars

and to the structure on the other end via calibrated load cell and heavy distribution beam.

The load on the structure at different floor levels was measured using load cells and the corresponding displacements were measured with the help of theodolites and LVDTs. Strain gauges were fixed on the reinforcement bars and concrete surface at critical locations on beams and columns. Total 96 strain gauges were fixed on the reinforcement of beams and columns as shown in Fig. 3. The numbers in the top row correspond to the strain gauges in Frame C (Fig. 1) and those in bottom row correspond to strain gauges in frame B. The left most column in Fig. 3 correspond to row 1 of columns (Fig. 1). The numbers outside the brackets correspond to strain gauges on the reinforcement towards the reader and the numbers in brackets correspond to the strain gauges on the opposite face.

5. Experimental results

The pushover curves as obtained for the structure while monitoring the displacement at various floor levels are shown in Fig. 4. The maximum total drift (approx 250 mm) is more than 4.5% of the total height of the structure. The inter-storey at failure between 1st and second storey was found to be around 5% of storey height and that between 2nd floor and roof was found to be around 3.6%.

The structure behaved linearly till a base shear value of around 50 kN. At this point the flexural tension cracks at the base of the columns started to get generated and the structure displayed a reduced stiffness. After reaching a base shear value of approx 110 kN, the cracks at the base of the columns opened wider and failures at other locations namely beams and beam-column joints started to show up. As a result the stiffness of the structure further went down, as can be seen from the pushover curves. After reaching the base shear values of 250 kN, the structure showed rapid degradation and it may be considered as the yield point with corresponding roof displacement of 68 mm. On further increase in the lateral load, the structure displayed a very soft behavior with large displacement increase for the same increase in the base shear. The peak base shear attained by the structure was 291 kN corresponding to roof displacement of 116 mm. Thereafter, the base shear

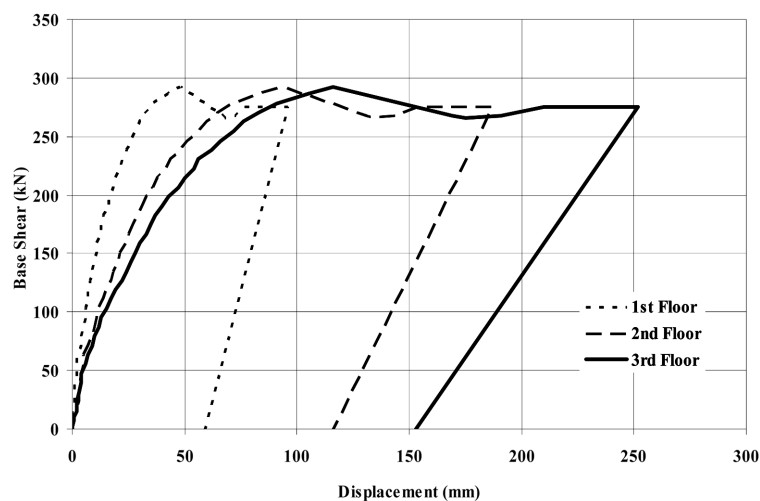


Fig. 4 Experimental pushover curves for the structure at different floor levels

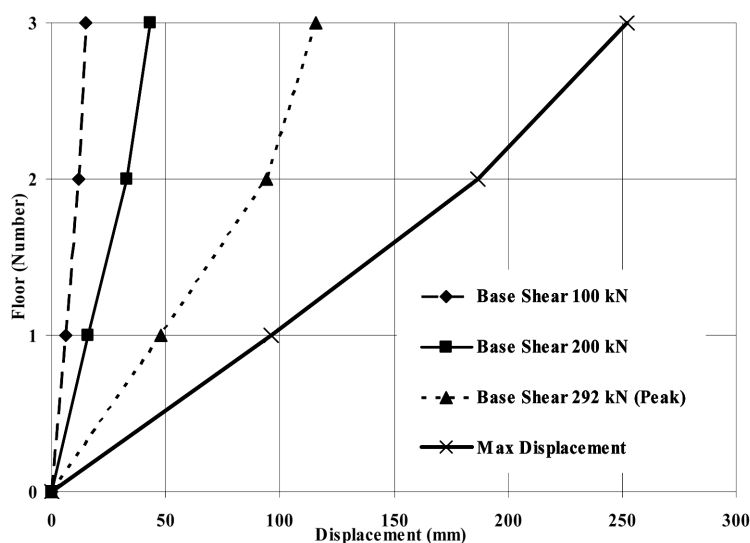


Fig. 5 Deflection profile of the structure at various stages of the test

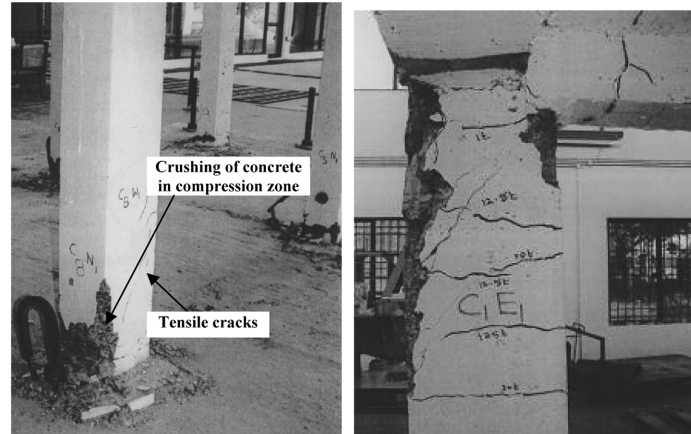
as monitored remains almost constant while the displacement increases rapidly. After reaching the total drift of 4.5%, the load was released and the unloading curve for the structure comes almost parallel to the loading curve thereby regaining the elastic part of the deflection. The inelastic roof deflection that could not be regained was found to be around 150 mm.

Fig. 5 shows the deflection profile of the structure at various stages of the test. The deflection profile clearly shows that as the lateral load on the structure was increased, the inter-storey drift increased and the structure went into inelastic (nonlinear) range. It was observed that in general, the inter-storey drift between second floor and roof is less than that between base and first floor and between first and second floor. The deflection profile of the structure clearly suggests that no soft storey mechanism at the first floor occurred, which may be attributed to the inelastic behaviour of the joints.

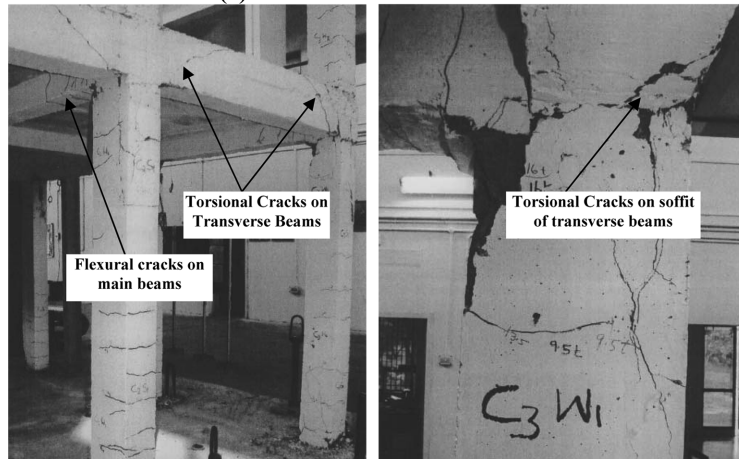
6. Failure patterns

Fig. 6 shows various failure modes and patterns observed during the experiment. Fig. 6(a) shows the flexural failure of columns that clearly shows crushing of concrete on compression face and tensile cracks on tension face. This is the result of combined axial force and uniaxial bending moment on the columns. As the lateral load was increased on the structure, columns underwent increasing axial forces combined with bending moment. Initially, the columns started to show tension cracks on the rear face. On further increase in the loads, these tension cracks grew further along the depth of the section demonstrating the shifting of neutral axis towards the compression face of the columns. Consequently, less area was available to resist higher compressive forces resulting in crushing of concrete on compression face of the column as shown in Fig. 6(a).

Fig. 6(b) shows the failure modes of the beam in flexural (for longitudinal, main beams) and torsional (for transverse beams) modes. Due to lateral loading, the bending moments were generated



(a) Flexural failure of columns



(b) Flexural and torsional failure of beams



(c) Joint shear failures

Fig. 6 Failure patterns observed in the experiment

in the longitudinal beams (beams running parallel to the loading direction) resulting in flexural tension cracks as shown in Fig. 6(b). Spalling of concrete was observed on the tension face of the beams. As the lateral load increased, the beams transverse to the direction of loading suffered large torsional moments. The beam depth was 200 mm while the same for the slab was 100 mm

Therefore the forces that were transferred through the plane of slabs resulted in torsional stresses in beams, resulting in typical torsional mode cracking of beams.

Fig. 6(c) shows joint shear failures observed in the structure. Under the action of lateral forces, beam-column joints are subjected to large shear stresses in the core. Typically, high bond stress requirements are also imposed on reinforcement bars entering into the joint. The axial and joint shear stresses result in principal tension and compression that leads to diagonal cracking and/or crushing of concrete in the joint core. The flexural forces from the beams and columns cause tension or compression forces in the longitudinal reinforcements passing through the joint. During plastic hinge formation, relatively large tensile forces are transferred through bond. When the longitudinal bars at the joint face are stressed beyond yield, splitting cracks are initiated along the bar at the joint face. If the cover to the reinforcement bars is less and if the joint core is not confined by confining reinforcement in the form of stirrups, the cover concrete is spalled off due to the pressure exerted by the beam reinforcement bars.

Fig. 6(c) shows the failure of exterior and interior joints of the structure. High stresses in the joint resulted in diagonal cracks in the core followed by cover spalling. In general, it is accepted that the exterior joints are more vulnerable under earthquake loads as compared to interior joints, and the same is verified in this test. Fig. 6(c) shows typical diagonal (shear) cracks in the joint. The diagonal cracks in the joints are formed due to principal tensile stresses generated as a result of axial and joint shear stresses. As the lateral forces were increased on the structure, the joint shear stress increased and in combination with the axial stresses, resulted in diagonal tension that was responsible for the development of diagonal tension cracks.

7. Strain readings

The experimentally observed strain values for the strain gauges 1, 2, 3 and 4 on column C1 (Fig. 1 and Fig. 3) are shown in Fig. 7. The plot clearly shows that as the base shear increased, the

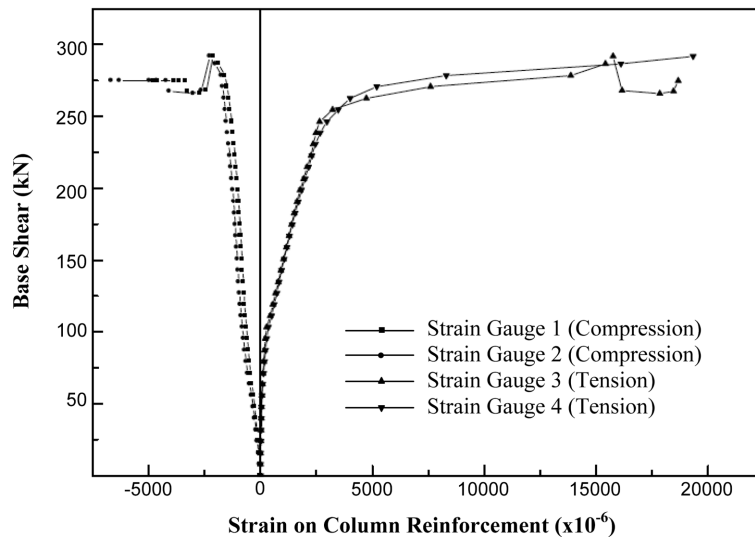


Fig. 7 Typical strains on column reinforcements

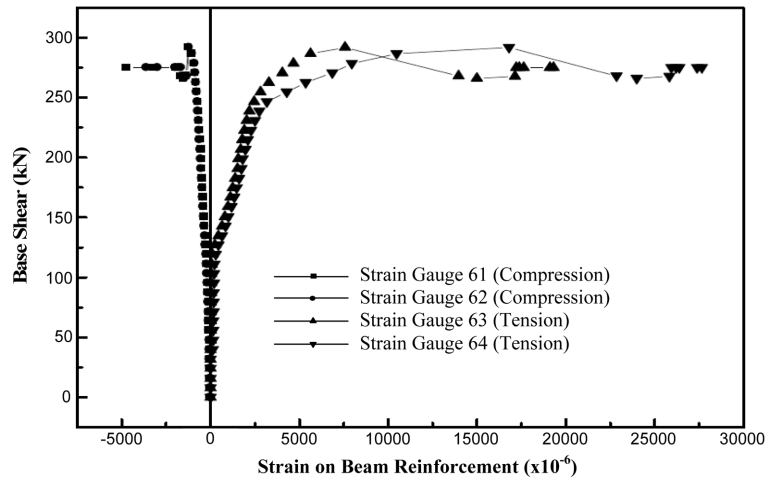


Fig. 8 Typical strains on beam reinforcements

column reinforcement strains increased almost linearly up to a base shear value of 250 kN and thereafter going in the non-linear range. The compression reinforcement recorded much less strains in comparison to tension reinforcement, which is as expected since in compression zone, concrete also contributes towards the resistance, whereas in tension zone, it does not. However, it can be seen that even the compression reinforcement yields beyond the base shear of around 275 kN.

The experimentally observed strain values for the strain gauges 61, 62, 63 and 64 on beam (Fig. 1 and Fig. 3) are shown in Fig. 8. The general behaviour of the strains in the beams is very similar to that for the columns. Again, the compression reinforcement recorded much less strains in comparison to tension reinforcement.

8. Analysis

The analysis of the structure was performed giving due considerations to the type of failure patterns observed in the test. It is generally observed that while performing a pushover analysis, mostly engineers consider only the flexural hinges. Since, it was observed in the experiment that the prominent failure modes were flexural failure of beams and columns, torsional failure of transverse beams and shear failure of joints, it was considered best to give due consideration to all three major failure modes. The approach followed for the analysis by the authors is described below.

9. Modeling of frame members (beams and columns), joints and slab (without non-linearities)

It is intuitive that modeling of members and joints using 3D solid elements and discrete bar elements with bond model will provide the results that will be much closer to reality (Sharma *et al.* 2008, 2009a). However, at the same time, it is understood that such a model is generally discouraged to be used in practice due to high modeling time and computational costs involved.

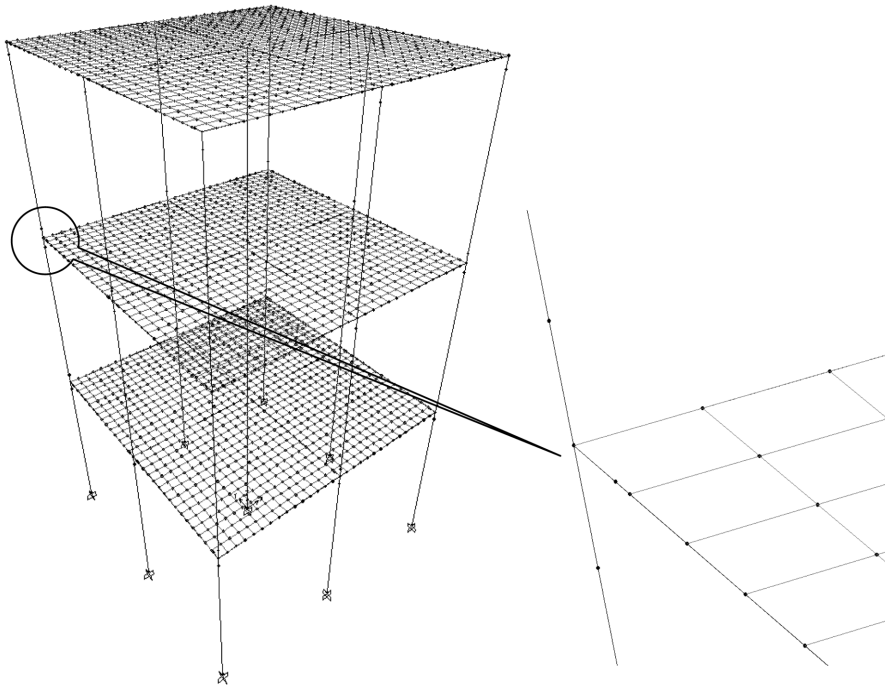


Fig. 9 Modeling of frame members, joints and slabs

Therefore, in order to provide a solution that is practical enough for usage in practice while being reasonably accurate, the beams and columns were modeled as 3D beam (frame) elements, with 6 degrees of freedom at both the nodes. Frame members are modeled as line elements connected at points (joints). However, actual structural members have finite cross-sectional dimensions. When two elements, such as a beam and column, are connected at a joint it has some finite dimensions due to overlap of the cross sections. The joint was modeled by dividing the frame elements into two parts having the same section dimensions. The slabs were modeled using the four node quadrilateral shell element. The model of the structure is shown in Fig. 9. The analysis was performed using commercial software SAP2000.

10. Modeling of nonlinearities

10.1 Flexural hinge

The stress-strain characteristics of a concrete confined by transverse reinforcement exhibits a more ductile behavior than its unconfined counterpart (Pauley and Priestley 1992, Park and Pauley 1975, Kent and Park 1971, Park *et al.* 1982). The first step, in order to generate moment-rotation characteristics for a section is therefore, to obtain the stress-strain curve for the confined concrete. Many researchers have proposed models to estimate the stress-strain curve for the confined concrete from mid twentieth century (Kent and Park 1971, Chan 1955, Baker and Amarakone 1964, Sargin *et al.* 1971) to late twentieth and early twenty first century (Park *et al.* 1982, Sheikh and Uzumeri

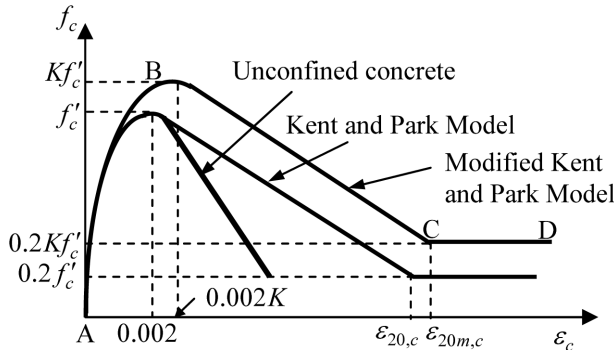


Fig 10 Stress-strain curve for concrete

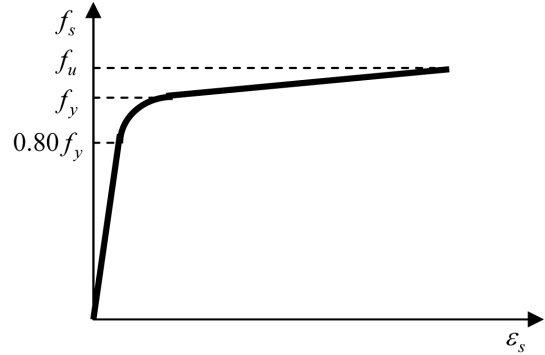


Fig 11 Stress-strain curve for reinforcement

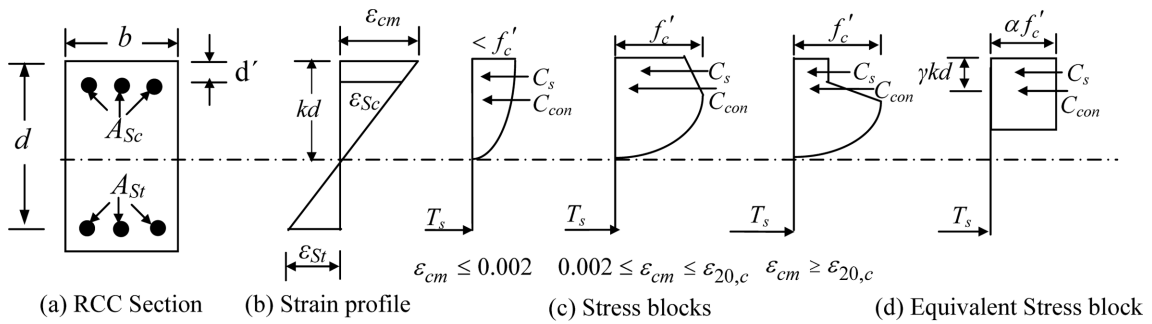


Fig. 12 Equivalent Stress blocks corresponding to different extreme compression fiber strain

1982, Mande *et al.* 1988, Rueda and Elnashai 1997, Li *et al.* 2005). Many other models also may be found in literature. However, out of all these models, the modified Kent and Park model (Park *et al.* 1982) and Mander model (Mander *et al.* 1988) are more popular, mainly because they offer a good balance between simplicity and accuracy. In this work, the modified Kent and Park model (Fig. 10) was followed, however the authors believe that the Mander model should also provide similar results. The stress-strain characteristics for the reinforcement steel used in this work considered strain hardening in the post yield portion of the curve (Fig. 11). Same curve was followed for reinforcement bars in tension and compression.

Once the stress-strain curves for steel and concrete are formulated, the moment-curvature characteristics of the section were derived using the standard procedure, where the concrete strain at the extreme compression fiber, ϵ_{cm} is assumed and the force equilibrium between compressive and tensile forces is established using iterative procedure to arrive at the correct neutral axis depth. The moment of resistance is then calculated by taking the moments of compressive and tensile forces about the centroid of the section and the corresponding curvature is obtained by dividing the extreme compression fiber strain by the neutral axis depth. In this work, the magnitude and point of application of compressive forces in concrete for various strain levels were calculated using the equivalent stress block approach (Fig. 12), since the sections were rectangular with constant width. The stress block parameter, α , and the neutral axis depth factor, γ , are calculated using following formulations.

$$\alpha = \frac{\int_0^{\epsilon_{cm}} f_c d\epsilon_c}{f'_c \epsilon_{cm}} \quad (1)$$

$$\gamma = 1 - \frac{\int_0^{\epsilon_{cm}} \epsilon_c f_c d\epsilon_c}{\epsilon_{cm} \int_0^{\epsilon_{cm}} f_c d\epsilon_c} \quad (2)$$

An in-house program was developed to obtain the characteristics. The moment-curvature characteristics thus generated were converted to moment-rotation characteristics using the following formulations.

Yield rotation,
$$\theta_y = \int_0^L \varphi_y dx = \int_0^L \frac{M_y}{EI} dx \quad (3)$$

And ultimate rotation,
$$\theta_u = \theta_y + (\varphi_u - \varphi_y)l_p \quad (4)$$

where, l_p is the plastic hinge length, which was calculated using the formulation suggested by Baker for confined concrete (Park and Pauley 1975, Baker and Amarakone 1964). Alternatively, the expression suggested by Pauley and Priestley (1992) may also be used. However, for typical beam and column proportions, a value of l_p as, half of effective depth of the section, may be used with sufficient accuracy.

The modulus of elasticity as E_c was considered as $4730(f'_c)^{0.5}$ (ACI 318 2008) and the cracked stiffness was considered by using modulus of elasticity as $0.5E_c$ (FEMA440 2005).

10.2 Shear hinge (shear force-deformation characteristics for members)

To predict the shear force versus deformation characteristics, an incremental analytical approach (Watanabe and Lee 1998) was followed. The model is based on the truss mechanism. In the analysis, the stirrup strain is gradually increased with a small increment and the resisting shear at each step is calculated. The stress state is characterized by a biaxial stress field in the concrete and a uniaxial tension field in the shear reinforcement. Kupfer and Bulicek (1991) theory for the equilibrium condition of stresses and compatibility condition of strains for the concrete element shown is followed. The equilibrium condition of stresses, compatibility condition of strains and constitutive laws are then used to obtain the complete shear force versus deformation characteristics for the members. The method is straightforward and easily programmable. However, a detailed description of the approach is beyond the scope of this paper and the details of the model may be obtained from the reference (Watanabe and Lee 1998). An in-house program was developed to obtain the characteristics.

10.3 Torsional hinge

The torsional hinge characteristics of the section were determined on the basis of Space Truss

analogy (Park and Paulay 1975). The cracking torsion, T_{cr} is calculated as

$$T_{cr} = 0.33 \sqrt{f'_c} (A_c^2 / P_c) \quad (5)$$

where,

f'_c = Standard Cylinder compressive strength of concrete, considered as 0.8 times the standard cube strength of concrete

A_c = Gross Area of concrete section in mm²

P_c = Perimeter of concrete section in mm

The ultimate torsional resistance, T_u of the section is calculated as

$$T_u = 2A_o A_{sv} f_{sv} \cot \theta / s_v \quad (6)$$

where,

A_o = gross area enclosed by shear flow path, considered as 0.85 times the area enclosed by centerline of the outermost closed transverse reinforcement

A_{sv} = Area of one leg of transverse reinforcement

f_{sv} = Yield/Ultimate stress of transverse reinforcement

s_v = centre to centre spacing of transverse reinforcement

The cracked stiffness of the section, $K_{t,cr}$ is considered as (Park and Pauley 1975)

$$K_{t,cr} = E_s (B_o D_o) 2A_{sv} \sqrt{m_f} / \{(B_o + D_o) s_v\} \quad (7)$$

where,

B_o = Shorter dimension of transverse reinforcement

D_o = Longer dimension of transverse reinforcement

E_s = Modulus of elasticity of transverse reinforcing steel

M_f = Ratio of yield stress of transverse reinforcement to that of longitudinal reinforcement

10.4 Joint hinge

As discussed earlier, the structure had suffered severe damages in the joint region, which is generally true for structures with non-seismic detailing subjected to earthquakes. Therefore, it is very important to model the nonlinearities in the beam-column joints in order to capture the real behavior of the structure. Also, it is true that a detailed modeling of the structure using 3D solid elements for concrete with an associated constitutive law, such as microplane model, with reinforcement modeled as bar elements and a specified bond characteristics is likely to give realistic results (Sharma *et al.* 2008, 2009a). However, such an analysis is extremely time consuming and therefore is discouraging for practitioners. Thus, a suitable model which can capture the true behavior of joints without making the problem too complex was looked for.

In the past, several attempts have been made to propose various models to capture the inelastic behavior of the beam-column joints and many researchers have attempted to model the behaviour of RC beam-column joints following various approaches that include, lumped plasticity models, multi-spring models, finite element simulations and fracture mechanics based approaches. However, in some cases, the models were not objective, in other cases they were very detailed and focused only at the sub-assembly level or they were too complex to be used at the structural level. Only a few models have been proposed that are simple enough to be used at the structural level and provide

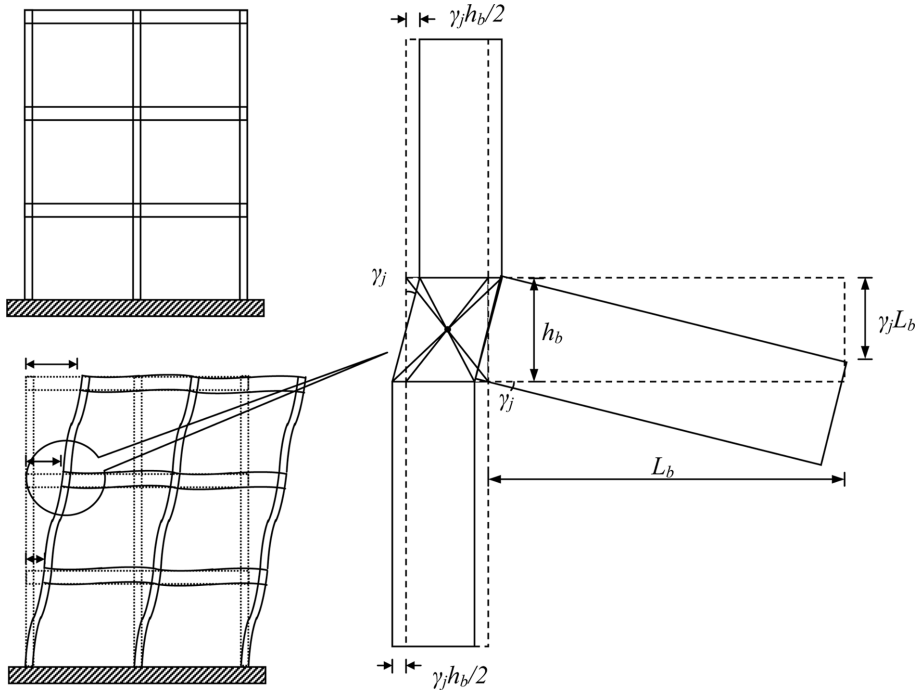


Fig. 13 Contribution of joint deformation to storey drift

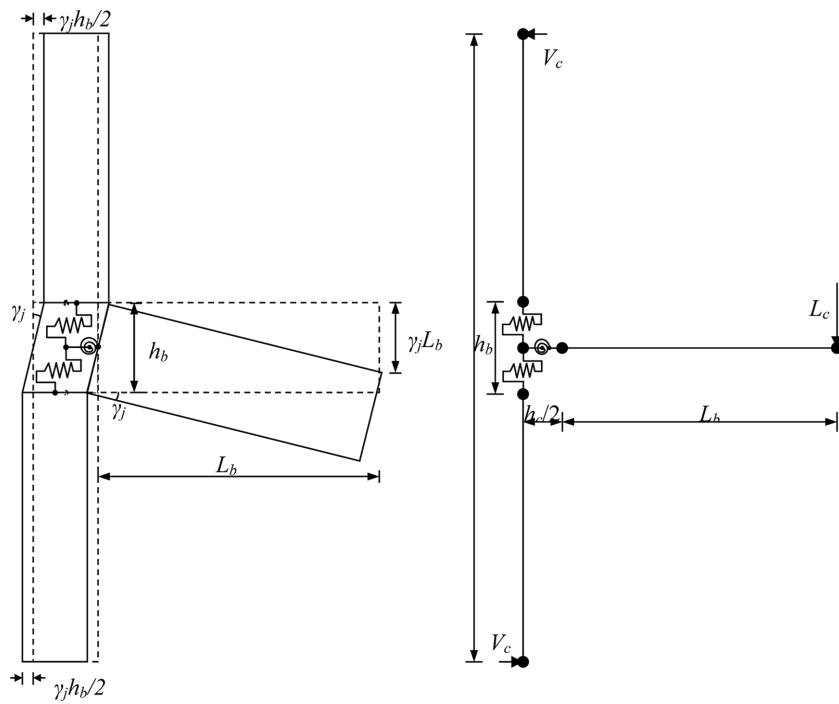


Fig. 14 Joint springs and implementation of the same in frame model

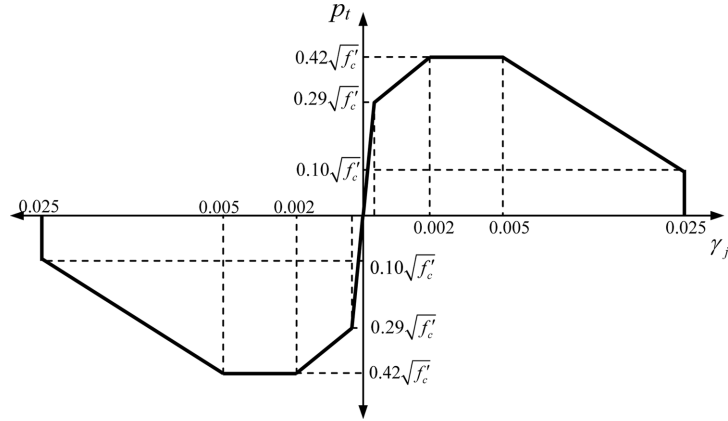


Fig. 15 Principal tensile stress-shear deformation relation used

results with reasonable accuracy. A detailed background of the models that had been proposed in the past with an emphasis on the strengths and limitations of the same is discussed by Sharma *et al.* (2009b, 2010). In this work, a new joint model proposed by Sharma *et al.* (2009b, 2010) is followed, which proved to be quite effective in capturing the realistic picture in case of poorly detailed beam-column joints. The model uses limiting principal tensile stress in the joint as the failure criteria so that due consideration is given to the axial load on the column. The spring characteristics are based on the actual deformations taking place in the sub-assembly due to joint shear distortion (Figs. 13 and 14).

For beam-column joints with the beam bars bent in the joint, the curve for principal tensile stress versus shear strain that was validated and used in this work is shown in Fig. 15. This curve is based on the recommendations by Priestley (1997). The joint characteristics are divided into one rotational spring characteristics assigned to beam part of the joint and two shear springs assigned to column part of the joint as shown in Fig. 8. The rotational and shear spring characteristics are derived using the relation shown in Fig. 9 and equilibrium criteria for the joints. The complete details on the procedure to determine the characteristics are given in (Sharma *et al.* 2009b, 2010).

11. Analytical model

Once the flexural hinge and shear characteristics for the beams and columns, torsional hinge characteristics for transverse beams and the joint characteristics in terms of flexural hinge for beam part and two shear hinges for column parts were determined, the same were assigned to the frame model of the structure. The total hinges assigned on a typical joint of the structure in the program and their physical significance are displayed in Fig. 16. As shown, the torsional hinges were assigned only to the beams with longitudinal axis transverse to the direction of loading while no other hinges were assigned to the same. For beams and columns, both flexural and shear hinges were assigned at the ends of the members while giving due consideration to the finite dimension of the joint. For the joint, two shear springs one for the column above and one for column below the joint and one flexural hinge for the beam framing into the joint were given. Since the loading was uni-directional, no joint hinges were provided for the transverse beams framing into the joint.

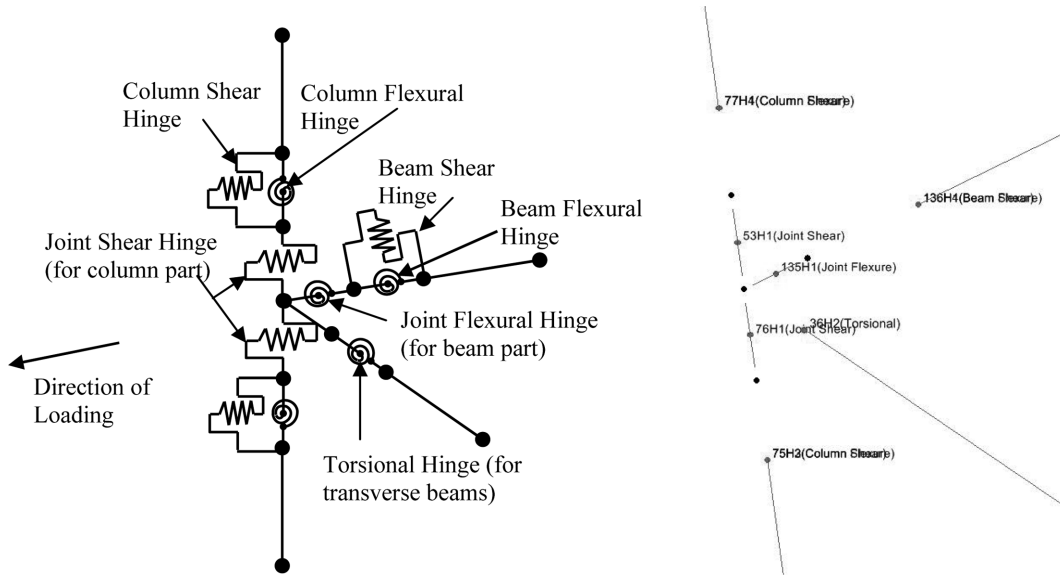


Fig. 16 Hinges assigned to the members and core of a typical joint

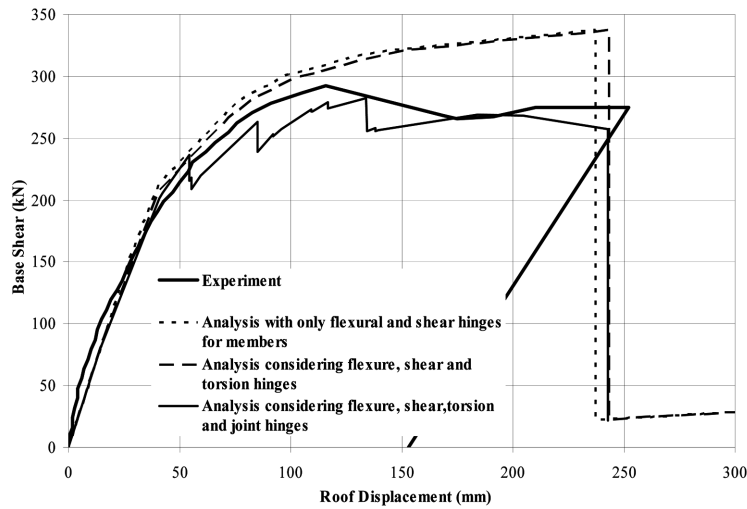


Fig. 17 Comparison of analytical and experimental results

12. Analysis results

Fig. 17 shows the comparison of experimental and analytical results. As shown in Fig. 17, three different analysis were performed for the model. In the first case, only the flexural and shear hinges were considered for the members. In the second case, additionally torsion hinges were considered and in the third case, joint hinges in addition to flexural, shear and torsional hinges were considered.

It can be seen that the model where only flexural and shear hinges were considered, initially follows the experimental curve very closely till yield, but thereafter over-predicts the strength of the

structure. The over-prediction of strength in the analysis results should be expected since the analysis considered only moment and shear hinges whereas in the experiment, it was found that the torsional and joint failure also contributed significantly towards base shear. However, in this case, the over-prediction of the base shear is not very high and even with such a simple and straight forward model, the analysis can be done with sufficient accuracy. However, it may not be always the case, especially in buildings with more pronounced eccentricity the joint failure.

After considering the torsional effects, the maximum base shear predicted analytically becomes just a bit different from the first case, and it does not improve the results very much. This shows that the torsional mode was not a major contributor to the behaviour of the structure. This can be confirmed by going back to Fig. 6(b) where it can be seen that the torsional cracks, though start appearing, are not fully developed. This shows that although the concrete starts cracking, the space truss of the reinforcement is sufficient to carry the torsional moment on the beams coming due to the loads.

The joint nonlinearities were modelled by introducing flexural and shear hinges for the beam and column portion of the joint respectively and calculating the characteristics as described earlier. The pushover curve of the structure obtained analytically while giving due consideration to joint nonlinearity in addition to flexural, shear and torsional hinges is shown in Fig. 17. As seen, after considering the joint characteristics, torsional effects, moment and shear characteristics the analysis results become very close to the experimental results. This is expected because in the experiments, joint shear failure was an important failure mode as observed.

Fig. 18 shows the analytically obtained deflected shape (scaled up) and failure patterns, while Fig. 19 shows a comparison of the experimentally observed and analytically simulated deflected shape of the structure. It can be observed that the displacement profile obtained from the analysis

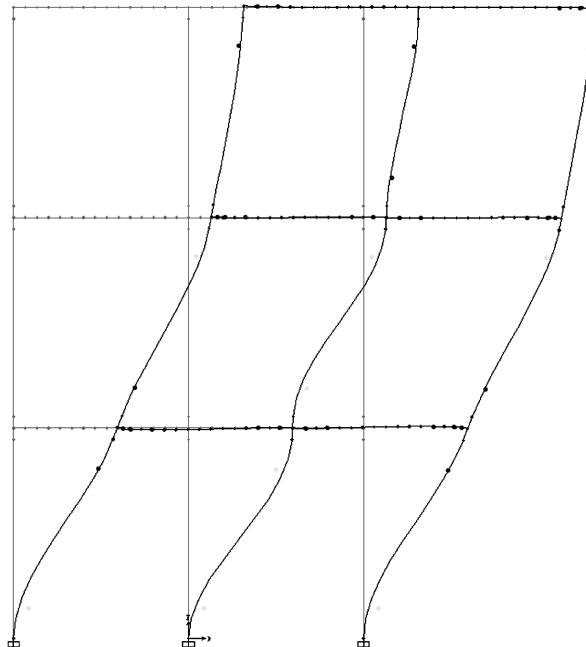


Fig. 18 Analytical deflected shape and failure pattern

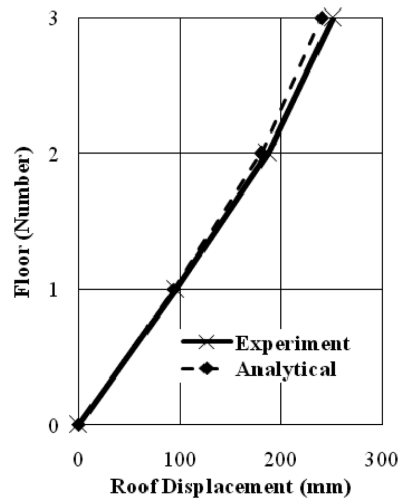


Fig. 19 Comparison of experimental and analytical deflected shape of the structure

matches closely with experimentally observed one. This further strengthens our viewpoint that with the proposed model, where the flexural, shear and torsional hinges for the members were modeled along with, very importantly, the joint hinges, could simulate almost all kinds of failure modes that were observed in the experiment and not only the base shear, but also the displacement demand at various storey levels and the complete displacement profile of the structure could be successfully captured.

13. Conclusions

A three storey-two bay reinforced concrete structure was tested under monotonically increasing lateral pushover loads with a parabolic loading pattern. The damage in the structure was found to be mostly concentrated in the form of flexural failures in beams and columns and joint shear failures. An attempt was made in order to analyze the structure with practically usable modeling techniques while at the same time being able to capture the failure modes displayed by the structure in the experiment. It was found from the analysis that modeling only the moment and shear hinges over predicted the results. After inclusion of joint characteristics, the model led to results in very close agreement with the experiment.

Acknowledgements

The authors highly acknowledge the efforts of Dr. N. Gopalakrishnan, Dr. K. Muthumani, Mr. A. Ramarao and the whole team of the ASTaR lab at SERC Chennai for successfully completing the experiment under BARC funded research project. The authors are also very thankful to Dr. A.K. Ghosh and Mr. H.S. Kushwaha for their encouragement and support throughout the project.

References

- ACI 318M-08 (2008), Building Code Requirements for Reinforced Concrete, *American Concrete Institute*, Detroit, Michigan.
- Antoniou, S. and Pinho, R. (2004), "Development and verification of a displacement-based adaptive pushover procedure", *J. Earthq. Eng.*, **8**(5), 643-661.
- Applied Technology Council (1996), "Seismic evaluation and retrofit of concrete buildings", Report No. ATC-40, Applied Technology Council, Redwood City, California.
- Applied Technology Council (2005), "Improvement of nonlinear static seismic analysis procedures", Report No. FEMA-440, Washington, D.C.
- Baker, A.L.L. and Amarakone, A.M.N. (1964), "Inelastic hyperstatic frames analysis", *Proceedings of the International Symposium on the Flexural Mechanics of Reinforced Concrete*, ASCE-ACI, Miami, November.
- Biddah, A. and Ghobarah, A. (1999), "Modelling of shear deformation and bond slip in reinforced concrete joints", *Struct. Eng. Mech.*, **7**(4), 413-432.
- Building Seismic Safety Council (1997), "NEHRP guidelines for the seismic rehabilitation of buildings", Report FEMA-273 (Guidelines) and Report FEMA-274 (Commentary), Washington, D.C.
- Chan, W.L. (1955), "The ultimate strength and deformation of plastic hinges in reinforced concrete frameworks", *Mag. Concrete Res.*, **7**(21), 121-132.
- Chopra, A.K. and Goel, R.K. (2002), "A modal pushover analysis procedure for estimating seismic demands for buildings", *Earthq. Eng. Struct. Dyn.*, **31**, 561-582.
- Chopra, A.K. and Goel, R.K. (2004), "A modal pushover analysis procedure to estimate seismic demands for unsymmetric-plan buildings", *Earthq. Eng. Struct. Dyn.*, **33**, 903-927.
- Cosenza, E., Manfredi, G. and Verderame, G.M. (2006), "A fibre model for push-over analysis of under-designed reinforced concrete frames", *Comput. Struct.*, **84**, 904-916.
- Fajfar, P. and Gasperic, P. (1996), "The N2 method for the seismic damage analysis of RC buildings", *Earthq. Eng. Struct. Dyn.*, **25**, 31-46.
- Fajfar, P. (2000), "A nonlinear analysis method for performance based seismic design", *Earthq. Spectra*, **16**(3), 573-592.
- FEMA (2000), "Prestandard and commentary for seismic rehabilitation of buildings", Report No. FEMA-356, Washington, D.C.
- Han, S.W. and Chopra, A.K. (2006), "Approximate incremental dynamic analysis using the modal pushover analysis procedure", *Earthq. Eng. Struct. Dyn.*, **35**, 1853-1873.
- Isakovic, T. and Fischinger, M. (2006), "Higher modes in simplified inelastic seismic analysis of single column bent viaducts", *Earthq. Eng. Struct. Dyn.*, **35**, 95-114.
- Kafrawy, O.E., Bagchi, A. and Humar, J. (2011), "Seismic performance of concrete moment resisting frame buildings in Canada", *Struct. Eng. Mech.*, **37**(2), 233-251.
- Kent, D.C. and Park, R. (1971), "Flexural members with confined concrete", *J. Struct. Div.-ASCE*, **97**(ST7), 1969-1990.
- Kilar, V. and Fajfar, P. (1996), "Simplified push-over analysis of building structure", *Proceedings of the Eleventh World Conference on Earthquake Engineering*, Paper 1011, Pergamon, Elsevier Science Ltd., Acapulco, México.
- Kilar, V. and Fajfar, P. (1997), "Simple push-over analysis of asymmetric buildings", *Earthq. Eng. Struct. Dyn.*, **26**, 233-249.
- Kilar, V. and Fajfar, P. (2001), "On the applicability of pushover analysis to the seismic performance evaluation of asymmetric buildings", *Eur. Earthq. Eng.*, **XV**(1), 20-31.
- Kunnath, S.K. (2004), "Identification of modal combination for nonlinear static analysis of building structures", *Comput-Aid. Civil Infrastruct. Eng.*, **19**, 246-259.
- Kupfer, H. and Bulicek, H. (1991), "A consistent model for the design of shear reinforcement in slender beams with I- or Box-shaped cross section", *International Workshop on Concrete Shear in Earthquake*, Houston, Tex.
- Li, Y.F., Chen, S.H., Chang, K.C. and Liu, K.Y. (2005), "A constitutive model of concrete confined by steel reinforcements and steel jackets", *Can. J. Civ. Eng.*, **32**, 279-288.
- Ludovico, M.D., Balsamo, A., Prota, A. and Manfredi, G. (2008), "Comparative assessment of seismic

- rehabilitation techniques on a full scale 3-story RC moment frame structure”, *Struct. Eng. Mech.*, **28**(6), 727-747.
- Mander, J.B., Priestley, M.J.N. and Park, R. (1988), Theoretical stress-strain behavior of confined concrete”, *J. Struct. Eng.-ASCE*, **114**(8), 1804-1826.
- Paraskeva, T.S., Kappos, A.J. and Sextos, A.G. (2006), “Extension of modal pushover analysis to seismic assessment of bridges”, *Earthq. Eng. Struct. Dyn.*, **35**, 1269-1293.
- Park, R. and Paulay, T. (1975), *Reinforced Concrete Structures*, John Wiley & Sons, New York.
- Park, R., Priestley, M.J.N. and Gill, W.D. (1982), “Ductility of square-confined concrete columns”, *J. Struct. Eng.-ASCE*, **108**(ST4), 929-950.
- Paulay, T. and Priestley, M.J.N. (1992), *Seismic Design of Reinforced Concrete and Masonry Buildings*, John Wiley and Sons, New York.
- Priestley, M.J.N. (1997), “Displacement based seismic assessment of reinforced concrete buildings”, *J. Earthq. Eng.*, **1**(1), 157-192.
- Rueda, J.E.M. and Elnashai, A.S. (1997), “Confined concrete model under cyclic load”, *Mater. Struct.*, **30**(3), 139-147.
- Samra, R.M. (1990), “Ductility analysis of confined columns”, *J. Struct. Eng.-ASCE*, **116**(11), 3148-3161.
- Sargin, M., Ghosh, S.K. and Handa, V.K. (1971), “Effects of lateral reinforcement upon the strength and deformation properties of concrete”, *Mag. Concrete Res.*, **23**(75-76), 99-110.
- Sharma, A., Reddy, G.R., Vaze, K.K., Ghosh, A.K., Kushwaha, H.S. and Eligehausen, R. (2008), “Investigations on inelastic behavior of non-seismically detailed reinforced concrete beam-column joints under cyclic excitations”, BARC External Report No. BARC/2008/E/017.
- Sharma, A., Genesio, G., Reddy, G.R. and Eligehausen, R. (2009a), “Nonlinear dynamic analysis using microplane model for concrete and bond slip model for prediction of behavior of non-seismically detailed RCC beam-column joints”, *J. Struct. Eng., SERC*, **36**(4), 250-257.
- Sharma, A., Reddy, G.R., Vaze, K.K., Ghosh, A.K., Kushwaha, H.S. and Eligehausen, R. (2009b), “Joint model to simulate inelastic shear behavior of poorly detailed exterior and interior beam-column connections reinforced with deformed bars under seismic excitations”, BARC External Report No. BARC/2009/E/026.
- Sharma, A., Eligehausen, R. and Reddy, G.R. (2011), “A new model to simulate joint shear behavior of poorly detailed beam-column connections in rc structures under seismic loads - Part I - Exterior Joints”, *Int. J. Eng. Struct.*, **33**, 1034-1051.
- Sheikh, S.A. and Uzumeri, S.M. (1982), “Analytical model for concrete confinement in tied columns”, *J. Struct. Div.-ASCE*, **108**(ST12), 2703-2722.
- Watanabe, F. and Lee, J.Y. (1998), “Theoretical prediction of shear strength and failure mode of reinforced concrete beams”, *ACI Struct. J.*, **95**(6), 749-757.
- Weng, Y.T., Lin, K.C. and Hwang, S.J. (2006), “Experimental and analytical performance assessment of in-situ pushover tests of school buildings in Taiwan”, *Proceedings of the 4th International Conference on Earthquake Engineering*, Taipei, Taiwan, Paper No. 154.
- Ziyaeifara, M. and Noguchib, H. (2000), “A refined model for beam elements and beam-column joints”, *Comput. Struct.*, **76**(4), 551-564.